RAMAN SPECTROSCOPY-BASED DIAGNOTSICS OF LYME DISEASE IN BLOOD

An Undergraduate Research Scholars Thesis

by

ROHINI MOREY

Submitted to the LAUNCH: Undergraduate Research office at
Texas A&M University
in partial fulfillment of requirements for the designation as an

UNDERGRADUATE RESEARCH SCHOLAR

Approved by
Faculty Research Advisors: Dmitry Kurouski Ph.D.
Artem Rogovskyy Ph.D.

May 2021

Major: Biochemistry

RESEARCH COMPLIANCE CERTIFICATION

Research activities involving the use of human subjects, vertebrate animals, and/or biohazards must be reviewed and approved by the appropriate Texas A&M University regulatory research committee (i.e., IRB, IACUC, IBC) before the activity can commence. This requirement applies to activities conducted at Texas A&M and to activities conducted at non-Texas A&M facilities or institutions. In both cases, students are responsible for working with the relevant Texas A&M research compliance program to ensure and document that all Texas A&M compliance obligations are met before the study begins.

I, Rohini Morey, certify that all research compliance requirements related to this Undergraduate Research Scholars thesis have been addressed with my Research Faculty Dr. Dmitry Kurouski and Dr. Artem Rogovskyy prior to the collection of any data used in this final thesis submission.

This project required approval from the Texas A&M University Research Compliance & Biosafety office.

TABLE OF CONTENTS

ABSTRACT

Raman Spectroscopy-based Diagnostics of Lyme's Disease in Blood

Rohini Morey
Department of Biochemistry and Biophysics
Texas A&M University

Research Faculty Advisor: Dmitry Kurouski Ph.D.
Department of Biochemistry & Biophysics
Texas A&M University

Research Faculty Advisor: Artem Rogovskyy Ph.D.
Department of Veterinary Pathobiology
Texas A&M University

Lyme Disease (LD) is reportedly the most widespread vector-borne disease in the continental US. The causative LD agent is the spirochetal bacterium, *Borreliella burgdorferi* (*Bb*), which is spread through *Ixodes* ticks. When untreated, early non-specific symptoms such as fever, chills, and rashes can give way to more extreme conditions such as dermatitis, arthritis, facial palsy (i.e., partial facial paralysis), and severe neurological disorders (e.g., meningitis). LD is often misdiagnosed due to the early flu-like symptoms and poor sensitivity of the only validated two-tiered serological testing. This thesis compiles, the results of two studies, which have examined the possibility of using Raman Spectroscopy (RS) as a diagnostic tool of LD. RS is a method that uses the excitation of particles to higher vibrational and rotational states to distinguish between different chemical structures. The first study involved infecting mice with

two wilt-type *Bb* strains (B31, 297) and one B31-derived mutant (ΔvIsE), and using a home-built confocal Raman microscope to acquire spectra of blood sampled from the mice prior to and after *Bb* infection. The Partial Least Squares- Discriminant analysis of the spectra resulted in detection of *Bb* mouse infection with 86% accuracy for 297, and with 89% accuracy for *Bb* B31 and ΔvIsE. The second study involved testing of human blood sampled from LD-confirmed and, and LD-negative (control) patients. The results showed that the True Positive Rate was 88-90%.

DEDICATION

I would like to begin this dedication, thanking my Principal Instructor and mentor Dr. Dmitry Kurouski for his faith in me and my abilities. He graciously allowed me to lead this project and has been of infinite help in the process of writing this thesis. I would also like to thank my graduate and undergraduate mentors, Charles Farber, who helped with the technological and analytical portion of the project, and Mark Krimmer, who trained me to work with the Surface Enhanced Raman Spectrometer and the blood samples.

ACKNOWLEDGEMENTS

Contributors

I would like to begin this dedication, thanking my Principal Instructor and mentor Dr. Dmitry Kurouski for his faith in me and my abilities. He graciously allowed me to lead this project and has been of infinite help in the process of writing this thesis. I would also like to thank my graduate and undergraduate mentors, Charles Farber, who helped with the technological and analytical portion of the project, and Mark Krimmer, who trained me to work with the Surface Enhanced Raman Spectrometer and the blood samples. And I would like to thank my team which included Samantha Higgins, Cameron Theime, Dillon Humpal and Stephen Parlamas who helped me with collecting spectra for this project. I would also like to thank other members of the lab for their constant patience and support.

Secondly, I am thanking Dr. Artem Rogovskyy and his associate Ms. Mahila Batool and also his team for collaborating with us on this project and providing the blood samples from his lab for us to scan and analyze.

Thirdly, for the Bacterial culture for the fully infectious wild-type Bb strains, 297 and B31-A3 (B31) strains were the generous gifts of Patti Rosa and Scott Samuels by the way to Troy Bankhead. The B31-A3 lp28-1Δvls (ΔvlsE) strain was generously gifted by Troy Bankhead.

Finally, I am thanking my friends and family for their constant love and support.

Funding Sources

This work was also made possible in part by Bay Area Lyme Foundation via the Emerging Leader Award. Its contents are solely the responsibility of the authors and do not necessarily represent the official views of the Bay Area Lyme Foundation.

NOMENCLATURE

LD	Lyme Disease
Bb	*Borrelia burgdorferi*
RS	Raman Spectroscopy
LC-MS	Liquid Chromatography - Mass Spectroscopy
EIA	Enzyme Immunoassay
IFA	Immunofluorescence Assay
PCR	Polymerase Chain Reaction
PLS-DA	Partial Least Squares- Discriminant Analysis
TPR	True Positive Rate

1. INTRODUCTION

1.1 Lyme Disease

Lyme Disease (LD) is the most commonly reported vector-borne disease in the United States.[1] In the Center for Disease Control's (CDC) report on the disease between 2008 and 2015, there were over 275,000 cases reported in the continental United States, with the geographical focal point being the Northeast, mid-Atlantic and upper Midwest regions.[1]

Structure and Infectivity of Lyme Borreliosis

Though there are many strains of Lyme Disease, there are three that infect humans. *Borrelia afzelii* or *Borrelia garinii* are mostly seen in Europe and Asia[2], while the strain found most often in the Western Hemisphere is *Borrelia burgdorferi* (Bb)[3]. These strains are eubacterial and part of the phylum Spirochetes.[4] They have a peptidoglycan cell wall with the fast-moving flagella.[4] Bb, which is also called stain 'wild-type B31', has a genome that has already been sequenced.[5,6] This genome does not encode a lot of proteins for anabolic or biosynthetic activity, and thus must depend on the host to function.[5,6] Another remarkable feature is that Bb does not need iron to grow (this has only been shown in vitro)[7], and thus might be able to thrive even when the host cell limits iron as a defense mechanism. Finally, its genome has no toxic proteins or other toxins. In this way we can conclude that B. Burgdorferi mostly infects by adhesion to cells and avoiding or building a defense for immune responses by the host cell.[4]

Lyme Disease in Humans

Lyme Disease was discovered as a novel disease in 1976, when multiple children in Lyme, Connecticut developed symptoms similar to juvenile rheumatoid arthritis.[8] However, it was later discovered that this is a vector-borne disease that is spread by the tick *Ixodus scapularis*.[9] Though, it is this tick that is often the vector of LD, its life cycle can follow through multiple avian and mammalian vectors and usually spreads during late spring to early summer.[10]

The disease develops in stages and has different manifestation of symptoms or remission and exacerbations depending on the stage of the disease.[8] Stage 1 usually lasts for a couple of days to a week, where a small localized infection develops at the site of the tick bite.[11,12] This infection has a characteristic shape and size, and is the way most preliminary diagnosis of LD occurs, which is then followed by serological blood tests.[13,14] Weeks later in Stage 2, the infection disseminates in the body and can cause irritation and skin lesions,[8,15] and months later it can manifest into neurological disorders[15] and arthritis[16,17], which is usually a hallmark of Stage 3. However, the infection symptoms can manifest differently from patient to patient.[1] Furthermore, regional variants exist based on the continent that the particular spirochete is found.[4,8]

Current Diagnostic Tests for Lyme Disease

The way most physicians recognize LD is through the characteristic rash that appears in Stage 1 of the disease. But after that there is an FDA approved two-tiered serological test what is performed to confirm the diagnosis.[14,18,19] The first tier can consist of either an Enzyme immunoassay (EIA) or an Immunofluorescence Assay (IFA); if this test is negative the second

test is rarely performed. The second tier of the test splits the patients into categories if whether the patient has had active symptoms for more than 30 days. If the patient has had symptoms for more than 30 days then an IgM and an IgG Western Blot is performed, if not then only an IgG Western blot is done.[20] To put it simply, this test detects the presence of antibodies present that have been created by the body to fight against the disease.

The drawback of this form of testing is that the accuracy is low, in the first three to four weeks of the disease when it progresses from Stage 1 to Stage 2.[19] This is either because the body has not yet created the antibodies to fight against the *Bb* or the disease has, for various reason, not disseminated properly in the body. The accuracy at these Stages in the disease accurately detects LD only 29 to 40% of the time.[19] It must be noted that when the Lyme disease progresses to stage three there is an 87% chance of detecting LD in patients exhibiting neurological defects and a 97% chance in accurately detecting LD in patients with arthritis.[14,19] Other issues include background seropositivity and cross reactivity with antigens that are not Bb.[21, 22]. Another study in Europe showed that when different methods of serological testing were performed in different labs, they resulted in conflicting diagnoses.[23] These tests also take about 1 to 2 weeks to process, precious time under which the patient's condition might worsen.[20]

Some other tests that are not federally approved are Polymerase Chain Reaction (PCR) tests, or bacterial culture tests.[14] Both have results that can vary based on strain of LD and progression of the disease in the patient's system. The PCR test tends to work best for the Wild-Type B31 strain, simply because this variant's DNA has been sequenced (one of the first spirochetes to be sequenced completely).[14,24] But with PCR, it is hard to keep up with emerging

strains, and the test itself can also be time consuming to process.[14,25,26] Bacterial cultures also pose different issues, with contamination and human error.[27] Both have between 70 to 80% accuracy in the later stages of the disease.[14]

Raman Spectroscopy

Introduction to Raman Spectroscopy

In order to find alternative diagnostic methods for LD, that are less laborious and time-consuming, this experiment delves into the possibility of using Raman Spectroscopy (RS). RS is proven to be a non-invasive and non-destructive diagnosis methods for a variety of different diseases, ranging from plant pathology[28,29] to detection of amyloid plaques in cerebrospinal fluid[31,32], forensic studies and explosives.[30] This form of spectroscopy is can be analyzed due to the inelastic Raman scattering of particles after the excitation of a molecule to different vibrational or rotational states,[32,33] which helps in identifying different vibrational bands within the molecule. Using the information acquired about the vibrational bands, one can deduce the important functional groups and the overall chemical make-up of the molecule being scanned.[32,33]

RS is a rapidly growing method to analyze and diagnose disease, that are often difficult to test the traditional route.[32,33] One of the successful examples of creating RS-based diagnostic tests include Rzyovika and colleagues who were able to detect metabolic changes in the blood which were characteristic of Alzheimer's disease.[34] RS has also proven to be specific to the disease as it was able to successfully distinguish between Alzheimer's and other forms of dementia.[31,32] Changes in blood composition due to Malaria[35] and other viral diseases[36] are also

conditions that RS has been successful at detecting. Using the paradigm that the previously mentioned groups had followed; RS was used to detect metabolic and chemical changes in LD.

Non-RS Spectroscopic Diagnostics for LD

In 2015, Molins and colleagues did a similar analysis of serum samples from patients with LD and a serologically negative group using liquid chromatography - mass spectroscopy (LC-MS)[37]. Molins and her colleagues were able to prove that the metabolic levels of 62 species had significantly increased while the levels of 32 species had decreased in serum samples. The species included cholesterol, cholesteryl acetate, phospholipids, sphingolipids, diacylglycerol, triglycerides and many other lipids and their derivatives.[37] This proves that there are some are a number of specific changes occurring in the blood, when a patient is infected with LD. However, despite having high sensitivity and specificity, it must also be noted that this form of testing is time-consuming as it requires many steps to be correctly processed. Therefore, this thesis presents RS as an alternative diagnostic test for the detection of LD.

2. METHODS

The whole project was divided into three distinct parts and were completed over the course of past two years. The first part involved working with blood collected from mice, which were injected with three different strains of the disease. The strains were the 'Wild-Type B31'[39] strain, the 'ΔvIsE' strain[40] and a novel '297'[41] strain.[38] The second development in this project was detecting LD in the blood samples of human patients, who all had the Bb strain, which is the strain found in the continental United States. We compared the 45 samples that tested positive through the two-tiered serological test to 35 samples that tested negative, and used them to create a standard Raman Spectra for a confirmed and negative LD blood respectively.

The materials and methods used for each of the sections of the project was similar. Some of the settings, such as the number of scans and the acquisition time, on the SERS had to be changed when transitioning from mouse blood to human blood.

Ethics Statements

Ethics Statements on Murine Samples

The mouse experimental procedures were approved by the Institutional Animal Care and Use Committee of Texas A&M University and performed in accordance with Public Health Service (PHS) Policy on Humane Care and Use of Laboratory Animals (2002), Guide for the

Care and Use of Agricultural Animals in Research and Teaching (2010), and Guide for the Care and Use of Laboratory Animals (2011).[38]

Ethic Statements on Human Samples

Human samples were acquired from the Lyme Disease Biobank (Portland, OR, USA).

Raman Spectroscopy on Murine Samples

Bacterial Culture

Liquid Barbour-Stoenner-Kelly II medium which were supplemented with 6% rabbit serum (BSK-II; Gemini Bio-Products, CA, US) was used to cultivate the spirochetes and incubated under 2.5% CO_2 and at 35°C. For the animal tissue culture, BSK-II was supplemented with 0.02 mg ml^{-1} phosphomycin, 2.5 mg ml^{-1} amphotericin B and 0.05 mg ml^{-1} rifampicin to prevent bacterial and fungal contamination.[38]

Inducing Murine Sepsis and Creating blood smears

Fifteen C3H/ HeJ (C3H) mice were sourced from Jackson Laboratories (ME, US). C3H are immunocompetent mice which have the ability to develop Bb- induced arthritis. This was useful, as previously discussed, many times the serological test is not able to accurately predict LD in the earlier stages, and thus having a visible marker is beneficial.[43] All the mice were male and between four to six weeks of age. Three groups of mice were created randomly, with five mice per group. The mice were put through a shot adaption period, which allowed for the mice to acclimatize to the laboratory environment, and were then inoculated with 1.1 x 10^4 cells of the Bb Spirochete.[38,42] Each mouse in each group was inoculated with a different strain which were

297, B31 and ΔvIsE, respectively. B31 and its isogenic variant ΔvIsE are part of the RST1 Lyme Disease class, while the 297 mutant belongs to the RST2 class.[44,45] These two classes represent a third of the Bb population in the United States.

The infections progression was tracked by harvesting and culturing 50 µl of blood and was verified using dark field microscopy. The blood was harvested from the maxillary bleed on day 7 post-infection (pi) and other tissues were sampled form the ear pinnae on day 28 pi and form the bladder, ear pinnae, heart and tibiotarsal joints on day 56 pi.[46] Fifty µl of blood was collected from each animal through a cheek bleed. on day 0, 3 and 7 and then collected every week from that point on (day 14, day 21 etc.) until day 56 pi. Each blood sample was transferred to a sterile Eppendorf tube and then a sterile -80°C freezer was used to properly store the blood. Then when the blood was transferred to a -4°C freezer to store near the Raman equipment, where they were quickly used to collect spectra. Blood Smears were collected by transferring 50 µl of blood on to the slide that was wrapped with foil and then kept to dry for one hour. Since a smear on glass would not interfere and distort the laser, the slides were wrapped in a foil before they were smeared.[38]

Raman Spectroscopy

A home-built confocal Raman microscope which has a 785 nm continuous laser (Nescel, NJ) was used to acquire the Raman spectra. The laser is focused onto an inverted microscope (Nikon TE-2000 U) by manipulating the laser through a series of mirrors and then the laser passes through a 50/50 beam splitter and is then focused onto the objective which has the dry blood by a 20x Nikon objective (NA = 0.45). The scattered light was directed to an IsoPlane

SCT 320 spectrograph (Princeton Instruments, NJ, USA), which was provided with a 600 groove/nm grating blazed at 750 nm. The objective had a laser power was ~5.7 mW and the acquisition time was 10 seconds per spectrum. The Raleigh scattering was filtered with a LP02-785RE-25 long-pass filter (Semrock, NY) before entering the spectrograph. PIXIS:400BR CCD (Princeton Instruments) received the spectrograph dispersed light. A H117P2TE (Prior, MA) which is a motorized stage which was controlled by a Prior Proscan II, was used to move the sample relative to the incident laser beam. For each Bb strain, there were approximately 50 spectra acquired from spatially non-overlapping locations on the blood smear for each time point and replicate combination. In this manner, there were a total of 5813 spectra were analyzed.

Statistical Analyses

MATLAB with the MATLAB addon PLS_Toolbox (for PLS_DA, Eigenvector Research, Inc., WA) were used to perform all the statistical analysis in this study. The preprocessed intensity values at certain prominent Raman Bands were used to conduct an Analysis of Variance or ANOVA and the differences the ANOVA reported are significant to the $p = 0.05$ level. Post-hoc testing was performed by using the Tukey HSD test, which was utilized to generate the 95% confidence intervals. The spectra first had to be corrected to the baseline by the Automatic Weighted Least Squares algorithm with a 6^{th} order polynomial and then the normalized to the total amount of spectra. Following this, the spectra were then further processed by mean centering them.

The differences between each Bb mutant/ variant and between the time points were determined using Partial least squares discriminant analysis (PLS-DA). The PLS-DA models

were constructed for each time point pairing for each Bb strain which meant there was a 10 x 10 matrix was constructed to show the differences between the time points. A total of 45 binary models were created for the matrix, (not hundred as some of models were repeats and others were self-comparisons). However, when creating the models an unnaturally high signal to noise ratio was noticed and thus a rolling average scheme was applied. Though this cost in the number of total spectra available, the noise to signal ratio was significantly decreased. The raw spectra were averaged together in groups of 5 or 6 spectra per average. The True Positive Rate [TPR] were collected from the PLS-DA models created from the averaged sets and analyzed.

Raman Spectroscopy on Human Samples

Collection of Samples

There were a total of 75 samples received; 45 which were confirmed cases and 35 which were serologically negative tests. These samples were received from the Lyme Disease Biobank in Portland WA. The samples were uncentrifuged whole blood and had EDTA additive as an anticoagulant. The samples were stores in sterile Eppendorf tube and kept in the -80°C freezer for long periods of time. Once the samples were ready to be scanned by the Raman microscope and were transferred to a -4°C freezer. The same procedure was used to create the blood smears on foil-wrapped slides.

Raman Spectroscopy

The home-built confocal microscope was used again for this experiment, which much of the same settings. The only settings that changed were power of the laser which was ~8.5 mW

and the acquisition time was 30 secs. Another thing that changed from the Murine Samples were that 100 spectra were taken per sample, instead of the original 50.

Statistical Analysis

Since statistical analysis of the human LD involved only distinguishing between infected and non-infected samples, only one model had to be made to account the one parameter was present (as opposed to being two for the murine samples). The same statistical software and preprocessing method was applied to the murine and human samples. The noise-to-signal ratio was slightly higher than the mouse samples so the samples had to be averaged in sets 9 to 11 spectra per mean set.

3. RESULTS

Results from Murine Samples

In order to analyze the utility of RS in the detection of LD in whole blood samples, strains of B31, ΔvlsE and 297 LD were inoculated into immunocompetent mice and blood samples were taken on day 0, day 3, day 7 pi and then every week after that until day 56 pi. From these samples, 50 Raman Spectra were taken for every sample, at approximately ~5.75 mW of power and had an accumulation time of 10 seconds. In the spectra, the bands highlighted red denote bands associated with heme groups, the peaks highlighted blue denote protein groups and the peaks highlighted yellow represent aromatic vibrations. The Statistical Analysis of these samples gave the following results

Raman Spectra and Band Assignments

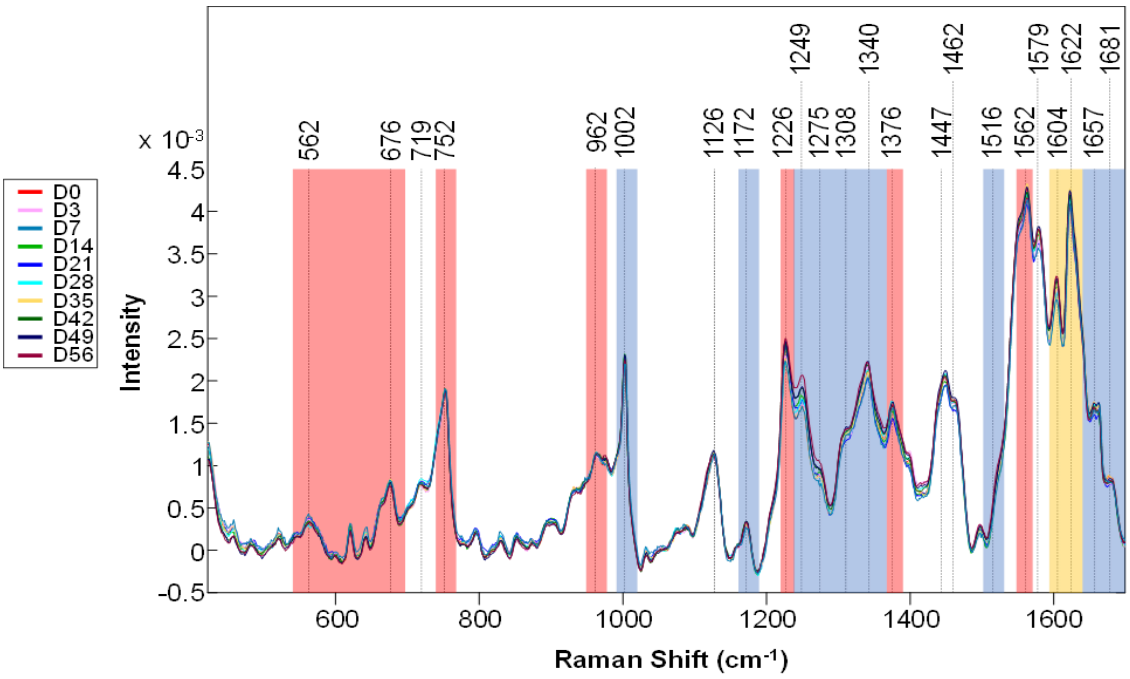

Figure 3.1: Averaged Raman spectra of blood samples taken from B. burgdorferi B31-infected C3H mice at all the examined time points post infection

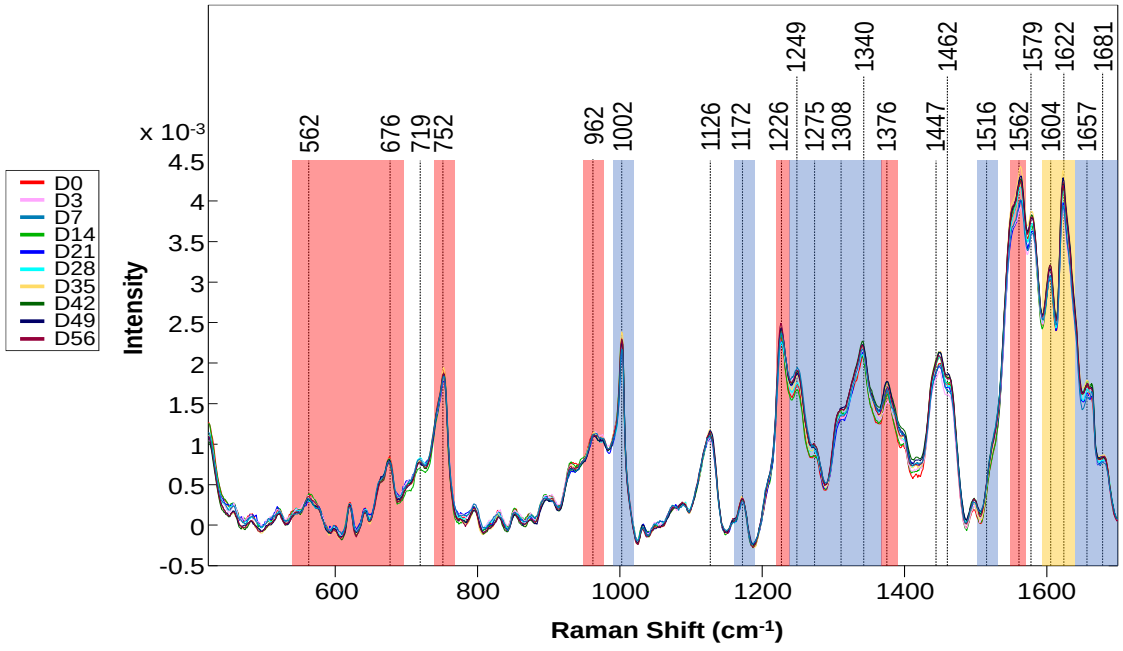

Figure 3.2: Averaged Raman spectra of blood samples taken from B. burgdorferi ΔvlsE-infected C3H mice at all the examined time points post infection.

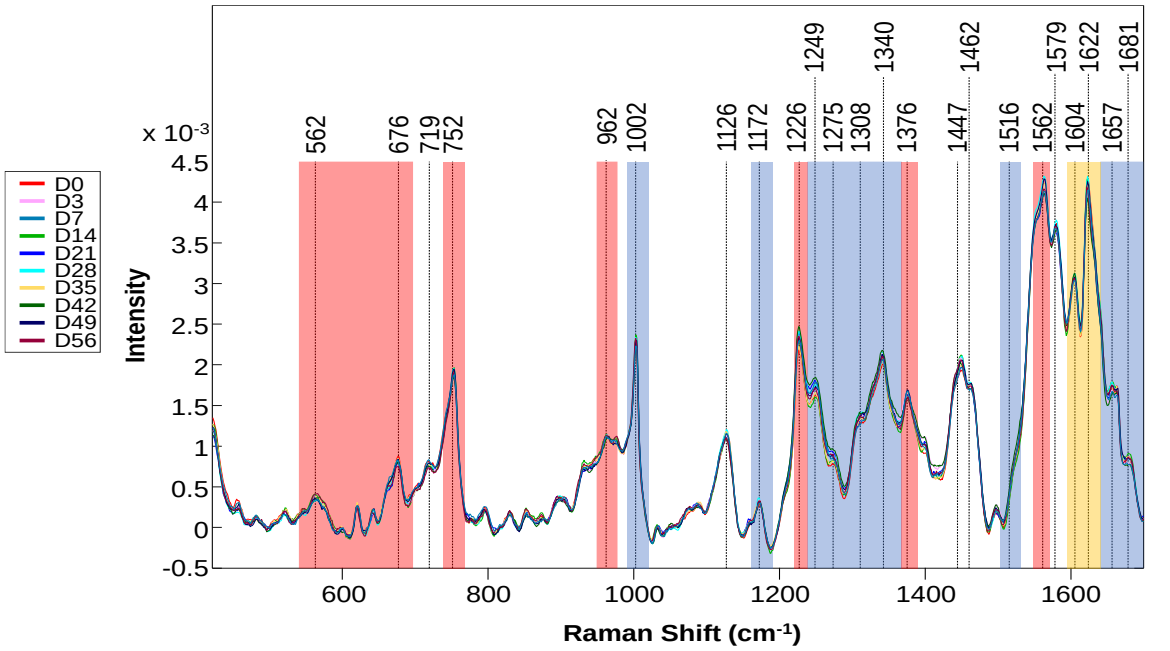

Figure 3.3: Averaged Raman spectra of blood samples taken from B. burgdorferi 297-infected C3H mice at all the examined time points post infection.

The spectra shown in Figure 3.1, Figure 3.2, and Figure 3.3 are the preprocessed, mean centered and averaged spectra. They are the wildtype B31, the isogenic ΔvlsE mutant and the 297 mutants from top to bottom. The most prominent and numerous vibrational band visible to the on the Raman Spectra are the bands that are associated with heme and protein structures, with some secondary peaks that represent other biomolecules such as sugars, aromatics and carotenoids. The red areas were representing the heme structure of the cell, while the blue represented the protein and the yellow was the aromatic vibrations. Table 3.1 shows the different peaks observed in the spectra and the vibrational bands they are assigned to.

Table 3.1: Assignment of spectral bands to different molecular vibrations and rotations

562	Fe-O_2 stretch (heme)[38,48]
676	Pyrrole symmetric bending (Heme)[38,48]
719	C–C–O related to glycosidic ring skeletal deformations[38,49]
752	Protein,[38,50] Heme ring breathing[38,48]
962	Associated with alpha CH of porphyrin ring[38,51]
1002	Phenylalanine ring breathing[36,38], CH_3 in-plane rocking of polyenes[36,38]
1126	C–C stretching[36,38]
1172	Trp, Phe[38,50]
1226	CH Bending (Heme)[38,48]
1249	*meso* CH of porphyrin ring[38,51]
1277	Lipids, Amide III[38,50]
1308	*meso* CH of porphyrin ring[38,47]
1340	Trp, Adenine, Lipids[38,50]
1376	Pyrrole ring[38,52]
1447	CH2[36,38]
1462	CH2, CH3[38,53]
1516	C=C[36,38]
1562	Conjugated CC stretching (heme)[38,48]
1579	C–C stretching[36,38]
1604	Aromatic ring[36,38]
1622	Aromatic ring[36,38]
1657	Amide I, C=C[38,54]
1681	Amide I,[38,53]carboxylic acids

Comparisons drawn from PLS-DA Models

The 10 x 10 matrices constructed by the PLS-DA models reported the True Positive Rate (TPR) for each pair of timepoints being compared. Table 3.2, Table 3.3 and Table 3.4 show the three matrices for each strain. The average TPR for the wildtype B31 and ΔvIsE strains were 89% while the 297 strain had a TPR of 86%.

Table 3.2: TPR Matrix for Wildtype B31

DAY	**0**	**3**	**7**	**14**	**21**	**28**	**35**	**42**	**49**	**56**
0	n/a	1	0.785	0.92	0.935	0.86	0.64	0.98	0.77	0.97
3	1	n/a	0.89	0.9	0.91	0.91	0.895	0.67	0.895	0.845
7	0.785	0.89	n/a	0.985	0.81	0.91	0.765	0.935	0.655	0.955
14	0.92	0.9	0.985	n/a	0.91	0.905	0.9	0.915	0.805	0.68
21	0.935	0.91	0.81	0.91	n/a	0.89	0.84	0.885	0.875	0.875
28	0.86	0.91	0.91	0.905	0.89	n/a	0.77	0.865	0.785	0.855
35	0.64	0.895	0.765	0.9	0.84	0.77	n/a	0.9	0.735	0.91
42	0.98	0.67	0.935	0.915	0.885	0.865	0.9	n/a	0.87	0.85
49	0.77	0.895	0.655	0.805	0.875	0.785	0.735	0.87	n/a	0.925
56	0.97	0.845	0.955	0.68	0.875	0.855	0.91	0.85	0.925	n/a

Table 3.3: TPR Matrix for 297 mutant

DAY	0	3	7	14	21	28	35	42	49	56
0	n/a	0.867	0.902	0.91	0.9	0.835	0.535	0.92	0.97	1
3	0.867	n/a	1	0.84	0.83	0.91	0.885	0.91	0.945	1
7	0.902	1	n/a	0.9	0.725	0.92	0.93	0.98	0.955	1
14	0.91	0.84	0.9	n/a	0.9	0.845	0.875	0.855	0.91	0.94
21	0.9	0.83	0.725	0.9	n/a	0.94	0.905	0.935	0.96	0.985
28	0.835	0.91	0.92	0.845	0.94	n/a	0.82	0.91	0.91	0.99
35	0.535	0.885	0.93	0.875	0.905	0.82	n/a	0.9	0.92	0.965
42	0.92	0.91	0.98	0.855	0.935	0.91	0.9	n/a	0.8	0.867
49	0.97	0.945	0.955	0.91	0.96	0.91	0.92	0.8	n/a	0.765
56	1	1	1	0.94	0.985	0.99	0.965	0.867	0.765	n/a

Table 3.4: TPR Matrix for the ΔvIsE mutant

DAY	0	3	7	14	21	28	35	42	49	56
0	n/a	0.84	0.685	0.81	0.875	0.76	0.925	0.955	0.91	0.84
3	0.84	n/a	0.775	0.855	0.89	0.895	0.975	0.965	0.96	0.945
7	0.685	0.775	n/a	0.895	0.765	0.78	0.98	1	0.905	0.97
14	0.81	0.855	0.895	n/a	0.945	0.8375	0.975	0.92	0.85	0.86
21	0.875	0.89	0.765	0.945	n/a	0.88	0.985	0.98	0.965	1
28	0.76	0.895	0.78	0.8375	0.88	n/a	0.98	0.985	0.96	0.985
35	0.925	0.975	0.98	0.975	0.985	0.98	n/a	0.77	0.906	0.77
42	0.955	0.965	1	0.92	0.98	0.985	0.77	n/a	0.82	0.7475
49	0.91	0.96	0.905	0.85	0.965	0.96	0.906	0.82	n/a	0.8
56	0.84	0.945	0.97	0.86	1	0.985	0.77	0.7475	0.8	n/a

There were two outliers observed at d0/d35, one in the wildtype B31 matrix which was 0.64 and the other in the mutant 297 which had a TPR of 0.535.

Results from Human Samples

Raman Spectra

Since mouse blood and human blood have similar components, it is observed in Figure 3.4 that similar peaks resurface from the human blood samples. The assignments of peaks to different vibrational bands are shown in table 1. However, some differences can be noted to the mouse spectra as the peaks 1249 cm^{-1} and 1277 cm^{-1} that denoted the meso porphyrin ring in the

center of the heme and Lipids (Amide III) respectively, have diminished significantly. Another difference is the diminished appearance of the peak that represents the carboxylic acids of Amide I (1681 cm^{-1}), the peak that denotes presence of CH_2 and CH_3 molecules (1460 cm^{-1}) and the peak that denotes the stretching of the carbon-carbon double bond (1516 cm^{-1}). All of these peaks appear as the shoulder of other peaks, so we cannot conclude that these molecular vibrations are not present in human blood samples, it could also imply that they were lost in the background.

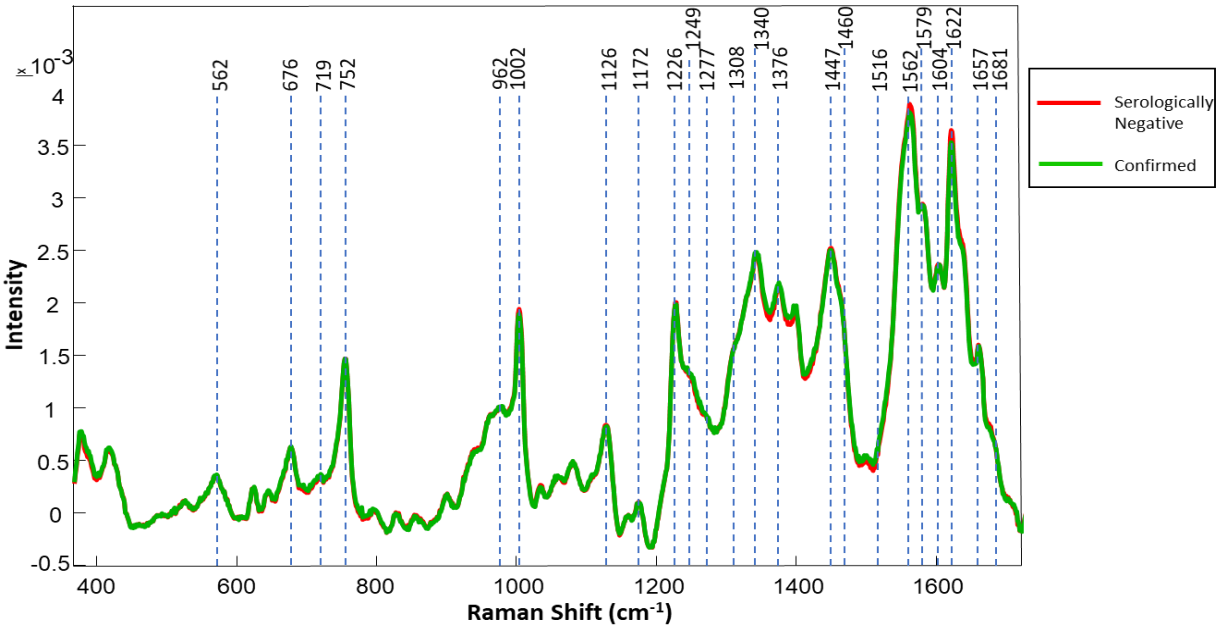

Figure 3.4: Averaged Raman spectra of blood samples taken from "confirmed" and "serologically negative" LD patients.

When the PLS-DA model compared the "Confirmed" samples to the "Serologically negative" samples, the following confusion matrix was obtained. This matrix, shown in Table

3.4, describes the number of spectra the model was able to accurately assign as either "Confirmed" or "Serologically Negative". The TPR describes the percentage of accurately ascribed spectra, thus showing how accurate the model is at predicting Lyme Disease. The model had an 88-90% success rate at correctly predicting the presence of LD in the blood samples. The total number of averaged samples in the confirmed group were 151 and the number of averaged spectra in the serologically negative group were 122.

Table 3.5: Confusion Matrix and TPR for the human blood samples that show the percent accuracy of the PLS-DA model in diagnosing LD

	Predicted as Confirmed	Predicted as Serologically Negative	TPR
Confirmed	134	12	***88.742%***
Serologically Negative	17	110	***90.164%***

4. CONCLUSION

Based on the results, it can be concluded that by using Raman Spectroscopy we can determine the presence of Lyme Disease in Blood Samples. For the Mouse Blood samples, the differences between the three variants of wildtype B31, isogenic ΔvlsE mutant and 297 mutants can be distinguished at an average percent accuracy of 89%, 89% and 86% respectively. It is also to be noted that we can observe high percent accuracy rates even in the beginning of the inoculation and not just 3 to 4 weeks after the samples had been infected, which is a drawback found in most LD testing today. For the human blood samples there was no method to track progression of LD, but the PLS-DA models were able to detect differences in the spectra to give a percent accuracy of 88 to 90%.

It is also important to note that no bands were found to be associated with the spirochete microbial family or the Bb pathogen itself. That implies that the confocal Raman Microscope was detecting the metabolic changes that the Bb pathogen causes in blood and not necessarily the pathogen itself. However, despite this, one can note the high percent accuracies in the first 7 days of the murine samples to observe that LD has a significant effect on the molecular make-up of the blood cells, in the early stages. Since mammalian blood is similar in nature, one could possibly expect the early stages of LD in humans to exhibit the same results. This form of symptomatic detection rather than pathogenic detection, can have drawbacks if other conditions have a similar effect on blood molecules as LD does, but to investigate that would require further testing.

REFERENCES

[1] Schwartz, A. M., Hinckley, A. F., Mead, P. S., Hook, S. A., & Kugeler, K. J. (2017). Surveillance for Lyme Disease - United States, 2008-2015. *MMWR Surveill Summ*, *66*(22), 1-12. https://doi.org/10.15585/mmwr.ss6622a1\

[2] Shapiro, E. D. (2014). Lyme Disease. *New England Journal of Medicine*, *370*(18), 1724-1731. https://doi.org/10.1056/NEJMcp1314325

[3] Pritt, B. S., Mead, P. S., Johnson, D. K. H., Neitzel, D. F., Respicio-Kingry, L. B., Davis, J. P., Schiffman, E., Sloan, L. M., Schriefer, M. E., Replogle, A. J., Paskewitz, S. M., Ray, J. A., Bjork, J., Steward, C. R., Deedon, A., Lee, X., Kingry, L. C., Miller, T. K., Feist, M. A., Theel, E. S., Patel, R., Irish, C. L., & Petersen, J. M. (2016). Identification of a novel pathogenic Borrelia species causing Lyme borreliosis with unusually high spirochaetaemia: a descriptive study. *Lancet Infect Dis*, *16*(5), 556-564. https://doi.org/10.1016/S1473-3099(15)00464-8

[4] Steere, A. C., Coburn, J., & Glickstein, L. (2004). The emergence of Lyme disease. *J Clin Invest*, *113*(8), 1093-1101. https://doi.org/10.1172/JCI21681

[5] Fraser CM, C. S., Huang WM, Sutton GG, Clayton R, Lathigra R, White O, Ketchum KA, Dodson R, Hickey EK, Gwinn M, Dougherty B, Tomb JF, Fleischmann RD, Richardson D, Peterson J, Kerlavage AR, Quackenbush J, Salzberg S, Hanson M, van Vugt R, Palmer N, Adams MD, Gocayne J, Weidman J, Utterback T, Watthey L, McDonald L, Artiach P, Bowman C, Garland S, Fuji C, Cotton MD, Horst K, Roberts K, Hatch B, Smith HO, Venter JC. (1997). Genomic sequence of a Lyme disease spirochaete, Borrelia burgdorferi. *Nature*, *390*, 580-586. https://doi.org/10.1038/37551

[6] Casjens, S., Palmer, N., van Vugt, R., Huang, W. M., Stevenson, B., Rosa, P., Lathigra, R., Sutton, G., Peterson, J., Dodson, R. J., Haft, D., Hickey, E., Gwinn, M., White, O., & Fraser, C. M. (2000). A bacterial genome in flux: the twelve linear and nine circular extrachromosomal DNAs in an infectious isolate of the Lyme disease spirochete Borrelia burgdorferi. *Mol Microbiol*, *35*(3), 490-516. https://doi.org/10.1046/j.1365-2958.2000.01698.x

[7] Posey, J. E., & Gherardini, F. C. (2000). Lack of a role for iron in the Lyme disease pathogen. *Science*, *288*(5471), 1651-1653. https://doi.org/10.1126/science.288.5471.1651

[8] Steere, A. C. (1989). Lyme disease. *N Engl J Med*, *321*(9), 586-596. https://doi.org/10.1056/NEJM198908313210906

[9] Spach, D. H., Liles, W. C., Campbell, G. L., Quick, R. E., Anderson, D. E., Jr, & Fritsche, T. R. . (1993). Tick-borne diseases in the United States. . *The New England journal of medicine*, *329*(13), 936-947. https://doi.org/10.1056/NEJM199309233291308

[10] Schwan, T. G., & Piesman, J. (2000). Temporal changes in outer surface proteins A and C of the lyme disease-associated spirochete, Borrelia burgdorferi, during the chain of infection in ticks and mice. *J Clin Microbiol*, *38*(1), 382-388. https://www.ncbi.nlm.nih.gov/pubmed/10618120

[11] Smith, R. P., Schoen, R. T., Rahn, D. W., Sikand, V. K., Nowakowski, J., Parenti, D. L., Holman, M. S., Persing, D. H., & Steere, A. C. (2002). Clinical characteristics and treatment outcome of early Lyme disease in patients with microbiologically confirmed erythema migrans. *Ann Intern Med*, *136*(6), 421-428. https://doi.org/10.7326/0003-4819-136-6-200203190-00005

[12] Steere, A. C., & Sikand, V. K. (2003). The presenting manifestations of Lyme disease and the outcomes of treatment. *N Engl J Med*, *348*(24), 2472-2474. https://doi.org/10.1056/NEJM200306123482423

[13] Steere, A. C., Sikand, V. K., Meurice, F., Parenti, D. L., Fikrig, E., Schoen, R. T., Nowakowski, J., Schmid, C. H., Laukamp, S., Buscarino, C., & Krause, D. S. (1998). Vaccination against Lyme disease with recombinant Borrelia burgdorferi outer-surface lipoprotein A with adjuvant. Lyme Disease Vaccine Study Group. *N Engl J Med*, *339*(4), 209-215. https://doi.org/10.1056/NEJM199807233390401

[14] Aguero-Rosenfeld ME, W. G., Schwartz I, Wormser GP. . (2005). Diagnosis of lyme borreliosis. *Clin Microbiol Rev*, *18*, 484-509. https://doi.org/10.1128/CMR.18.3.484-509.2005

[15] Duray PH, S. A. (1988). Clinical pathologic correlations of Lyme disease by stage. *Ann N Y Acad Sci*, *539*, 65-79. https://doi.org/10.1111/j.1749-6632.1988.tb31839.x.

[16] Steere, A. C., Schoen, R. T., & Taylor, E. (1987). The clinical evolution of Lyme arthritis. *Ann Intern Med*, *107*(5), 725-731. https://doi.org/10.7326/0003-4819-107-5-725

[17] Brown, C. R., Blaho, V. A., & Loiacono, C. M. (2003). Susceptibility to experimental Lyme arthritis correlates with KC and monocyte chemoattractant protein-1 production in joints and requires neutrophil recruitment via CXCR2. *J Immunol*, *171*(2), 893-901. https://doi.org/10.4049/jimmunol.171.2.893

[18] Lindsay, L. R., Bernat, K., & Dibernardo, A. (2014). Laboratory diagnostics for Lyme disease. *Can Commun Dis Rep*, *40*(11), 209-217. https://doi.org/10.14745/ccdr.v40i11a02

[19] Waddell, L. A., Greig, J., Mascarenhas, M., Harding, S., Lindsay, R., & Ogden, N. (2016). The Accuracy of Diagnostic Tests for Lyme Disease in Humans, A Systematic Review and Meta-Analysis of North American Research. *PLOS ONE*, *11*(12), e0168613. https://doi.org/10.1371/journal.pone.0168613

[20] Recommendations for test performance and interpretation from the Second National Conference on Serologic Diagnosis of Lyme Disease. (1995). *MMWR Morb Mortal Wkly Rep*, *44*(31), 590-591.

[21] Hilton, E., DeVoti, J., Benach, J. L., Halluska, M. L., White, D. J., Paxton, H., & Dumler, J. S. (1999). Seroprevalence and seroconversion for tick-borne diseases in a high-risk population in the northeast United States. *Am J Med*, *106*(4), 404-409. https://doi.org/10.1016/s0002-9343(99)00046-7

[22] Bacon, R. M., Biggerstaff, B. J., Schriefer, M. E., Gilmore, R. D., Jr., Philipp, M. T., Steere, A. C., Wormser, G. P., Marques, A. R., & Johnson, B. J. (2003). Serodiagnosis of Lyme disease by kinetic enzyme-linked immunosorbent assay using recombinant VlsE1 or peptide antigens of Borrelia burgdorferi compared with 2-tiered testing using whole-cell lysates. *J Infect Dis*, *187*(8), 1187-1199. https://doi.org/10.1086/374395

[23] Lager, M., Dessau, R. B., Wilhelmsson, P., Nyman, D., Jensen, G. F., Matussek, A., Lindgren, P. E., Henningsson, A. J., Baqir, H., Serrander, L., Johansson, M., Tjernberg, I., Skarstein, I., Ulvestad, E., Grude, N., Pedersen, A. B., Bredberg, A., Veflingstad, R., Wass, L., Aleke, J., Nordberg, M., Nyberg, C., Perander, L., Bojesson, C., Sjöberg, E., Lorentzen Å, R., Eikeland, R., Noraas, S., Henriksson, G. A., & Petrányi, G. (2019). Serological diagnostics of Lyme borreliosis: comparison of assays in twelve clinical laboratories in Northern Europe. *Eur J Clin Microbiol Infect Dis*, *38*(10), 1933-1945. https://doi.org/10.1007/s10096-019-03631-x

[24] Lee, S. H., Vigliotti, J. S., Vigliotti, V. S., Jones, W., & Shearer, D. M. (2014). Detection of borreliae in archived sera from patients with clinically suspect Lyme disease. *Int J Mol Sci*, *15*(3), 4284-4298. https://doi.org/10.3390/ijms15034284

[25] Nolte, O. (2012). Nucleic Acid Amplification Based Diagnostic of Lyme (Neuro-)borreliosis - Lost in the Jungle of Methods, Targets, and Assays? *Open Neurol J*, *6*, 129-139. https://doi.org/10.2174/1874205x01206010129

[26] Bil-Lula, I., Matuszek, P., Pfeiffer, T., & Woźniak, M. (2015). Lyme Borreliosis--the Utility of Improved Real-Time PCR Assay in the Detection of Borrelia burgdorferi Infections. *Adv Clin Exp Med*, *24*(4), 663-670. https://doi.org/10.17219/acem/28625

[27] Coulter, P., Lema, C., Flayhart, D., Linhardt, A. S., Aucott, J. N., Auwaerter, P. G., & Dumler, J. S. (2005). Two-year evaluation of Borrelia burgdorferi culture and supplemental tests for definitive diagnosis of Lyme disease. *J Clin Microbiol*, *43*(10), 5080-5084. https://doi.org/10.1128/jcm.43.10.5080-5084.2005

[28] Farber, C., Mahnke, M., Sanchez, L., & Kurouski, D. (2019). Advanced spectroscopic techniques for plant disease diagnostics. A review. *TrAC Trends in Analytical Chemistry*, *118*, 43-49. https://doi.org/https://doi.org/10.1016/j.trac.2019.05.022

[29] Farber, C., Bryan, R., Paetzold, L., Rush, C., & Kurouski, D. (2020). Non-Invasive Characterization of Single-, Double- and Triple-Viral Diseases of Wheat With a Hand-Held Raman Spectrometer [Original Research]. *Frontiers in Plant Science*, *11*(1300). https://doi.org/10.3389/fpls.2020.01300

[30] Esparza, I., Wang, R., & Kurouski, D. (2019). Surface-Enhanced Raman Analysis of Underlaying Colorants on Redyed Hair. *Analytical Chemistry*, *91*(11), 7313-7318. https://doi.org/10.1021/acs.analchem.9b01021

[31] Kurouski, D. (2016). Supramolecular Organization of Amyloid Fibrils.

[32] Kurouski, D., Van Duyne, R. P., & Lednev, I. K. (2015). Exploring the structure and formation mechanism of amyloid fibrils by Raman spectroscopy: a review. *Analyst*, *140*(15), 4967-4980. https://doi.org/10.1039/c5an00342c

[33] Ralbovsky, N. M., & Lednev, I. K. (2020). Towards development of a novel universal medical diagnostic method: Raman spectroscopy and machine learning. *Chem Soc Rev*, *49*(20), 7428-7453. https://doi.org/10.1039/d0cs01019g

[34] Ryzhikova, E., Kazakov, O., Halamkova, L., Celmins, D., Malone, P., Molho, E., Zimmerman, E. A., & Lednev, I. K. (2015). Raman spectroscopy of blood serum for Alzheimer's disease diagnostics: specificity relative to other types of dementia. *J Biophotonics*, *8*(7), 584-

596. https://doi.org/10.1002/jbio.201400060

[35] Hobro, A. J., Konishi, A., Coban, C., & Smith, N. I. (2013). Raman spectroscopic analysis of malaria disease progression via blood and plasma samples. *Analyst*, *138*(14), 3927-3933. https://doi.org/10.1039/c3an00255a

[36] Khan, S., Ullah, R., Saleem, M., Bilal, M., Rashid, R., Khan, I., Mahmood, A., & Nawaz, M. (2016). Raman spectroscopic analysis of dengue virus infection in human blood sera. *Optik*, *127*(4), 2086-2088. https://doi.org/https://doi.org/10.1016/j.ijleo.2015.11.060

[37] Molins, C. R., Ashton, L. V., Wormser, G. P., Hess, A. M., Delorey, M. J., Mahapatra, S., Schriefer, M. E., & Belisle, J. T. (2015). Development of a metabolic biosignature for detection of early Lyme disease. *Clin Infect Dis*, *60*(12), 1767-1775. https://doi.org/10.1093/cid/civ185

[38] Farber, C., Morey, R., Krimmer, M., Kurouski, D., & Rogovskyy, A. S. (2021). Exploring a possibility of using Raman spectroscopy for detection of Lyme disease. *J Biophotonics*, e202000477. https://doi.org/10.1002/jbio.202000477

[39] Elias, A. F., Stewart, P. E., Grimm, D., Caimano, M. J., Eggers, C. H., Tilly, K., Bono, J. L., Akins, D. R., Radolf, J. D., Schwan, T. G., & Rosa, P. (2002). Clonal polymorphism of Borrelia burgdorferi strain B31 MI: implications for mutagenesis in an infectious strain background. *Infect Immun*, *70*(4), 2139-2150. https://doi.org/10.1128/iai.70.4.2139-2150.2002

[40] Bankhead, T., & Chaconas, G. (2007). The role of VlsE antigenic variation in the Lyme disease spirochete: persistence through a mechanism that differs from other pathogens. *Mol Microbiol*, *65*(6), 1547-1558. https://doi.org/10.1111/j.1365-2958.2007.05895.x

[41] Hughes, C. A., Kodner, C. B., & Johnson, R. C. (1992). DNA analysis of Borrelia burgdorferi NCH-1, the first northcentral U.S. human Lyme disease isolate. *J Clin Microbiol*, *30*(3), 698-703. https://doi.org/10.1128/jcm.30.3.698703.1992

[42] Rogovskyy, A. S., Gillis, D. C., Ionov, Y., Gerasimov, E., & Zelikovsky, A. (2017). Antibody Response to Lyme Disease Spirochetes in the Context of VlsE-Mediated Immune Evasion. *Infection and Immunity*, *85*(1), e00890-00816. https://doi.org/10.1128/iai.00890-16

[43] Barthold, S. W., Beck, D. S., Hansen, G. M., Terwilliger, G. A., & Moody, K. D. (1990). Lyme borreliosis in selected strains and ages of laboratory mice. *J Infect Dis*, *162*(1), 133-138. https://doi.org/10.1093/infdis/162.1.133

[44] Liveris, D., Varde, S., Iyer, R., Koenig, S., Bittker, S., Cooper, D., McKenna, D., Nowakowski, J., Nadelman, R. B., Wormser, G. P., & Schwartz, I. (1999). Genetic diversity of Borrelia burgdorferi in lyme disease patients as determined by culture versus direct PCR with clinical specimens. *J Clin Microbiol*, *37*(3), 565-569. https://doi.org/10.1128/jcm.37.3.565-569.1999

[45] Liveris, D., Wormser, G. P., Nowakowski, J., Nadelman, R., Bittker, S., Cooper, D., Varde, S., Moy, F. H., Forseter, G., Pavia, C. S., & Schwartz, I. (1996). Molecular typing of Borrelia burgdorferi from Lyme disease patients by PCR-restriction fragment length polymorphism analysis. *J Clin Microbiol*, *34*(5), 1306-1309. https://doi.org/10.1128/jcm.34.5.1306-1309.1996

[46] Rogovskyy, A. S., Casselli, T., Tourand, Y., Jones, C. R., Owen, J. P., Mason, K. L., Scoles, G. A., & Bankhead, T. (2015). Evaluation of the Importance of VlsE Antigenic Variation for the Enzootic Cycle of Borrelia burgdorferi. *PLOS ONE*, *10*(4), e0124268. https://doi.org/10.1371/journal.pone.0124268

[47] LaRocca, T. J., & Benach, J. L. (2008). The important and diverse roles of antibodies in the host response to Borrelia infections. *Curr Top Microbiol Immunol*, *319*, 63-103. https://doi.org/10.1007/978-3-540-73900-5_4

[48] Casella, M., Lucotti, A., Tommasini, M., Bedoni, M., Forvi, E., Gramatica, F., & Zerbi, G. (2011). Raman and SERS recognition of β-carotene and haemoglobin fingerprints in human whole blood. *Spectrochim Acta A Mol Biomol Spectrosc*, *79*(5), 915-919. https://doi.org/10.1016/j.saa.2011.03.048

[49] Krimmer, M., Farber, C., & Kurouski, D. (2019). Rapid and Noninvasive Typing and Assessment of Nutrient Content of Maize Kernels Using a Handheld Raman Spectrometer. *ACS Omega*, *4*(15), 16330-16335. https://doi.org/10.1021/acsomega.9b01661

[50] Pichardo-Molina, J. L., Frausto-Reyes, C., Barbosa-García, O., Huerta-Franco, R., González-Trujillo, J. L., Ramírez-Alvarado, C. A., Gutiérrez-Juárez, G., & Medina-Gutiérrez, C. (2007). Raman spectroscopy and multivariate analysis of serum samples from breast cancer patients. *Lasers Med Sci*, *22*(4), 229-236. https://doi.org/10.1007/s10103-006-0432-8

[51] Lemler, P., Premasiri, W. R., DelMonaco, A., & Ziegler, L. D. (2014). NIR Raman spectra of whole human blood: effects of laser-induced and in vitro hemoglobin denaturation. *Anal Bioanal Chem*, *406*(1), 193-200. https://doi.org/10.1007/s00216-013-7427-7

[52] Atkins, C. G., Buckley, K., Blades, M. W., & Turner, R. F. B. (2017). Raman Spectroscopy of Blood and Blood Components. *Appl Spectrosc*, *71*(5), 767-793. https://doi.org/10.1177/0003702816686593

[53] Farber, C., Sanchez, L., Rizevsky, S., Ermolenkov, A., McCutchen, B., Cason, J., Simpson, C., Burow, M., & Kurouski, D. (2020). Raman Spectroscopy Enables Non-Invasive Identification of Peanut Genotypes and Value-Added Traits. *Sci Rep*, *10*(1), 7730. https://doi.org/10.1038/s41598-020-64730-w